

Experimental Studies with a Continually Online Trained Artificial Neural Network Controller for a Turbogenerator

^{1,2}Ganesh K Venayagamoorthy, *Member, IEEE*, and ^{1,3}Ronald G Harley, *Fellow, IEEE*

¹Department of Electrical Engineering, University of Natal, Durban 4041, South Africa

²Department of Electronic Engineering, M L Sultan Technikon, Durban, South Africa

³School of Electrical and Computer Engineering, Georgia Institute of Technology, Atlanta, USA

email: gkumar@saiee.org.za & harley@eng.und.ac.za

Abstract

This paper presents the design of a Continually Online Trained (COT) Artificial Neural Network (ANN) controller for a laboratory turbogenerator system connected to the infinite bus through a transmission line in real time. Two COT ANNs are used for the implementation; one ANN to identify the complex nonlinear dynamics of the power system and the other ANN to control the turbogenerator. Practical results are presented to show that COT ANN controllers can control turbogenerators under steady state as well as transient conditions in the laboratory environment.

Introduction

Turbogenerators supply most of the electrical energy produced by mankind and therefore form major components in electric power systems and their performance is directly related to security and stability of power system operation. A turbogenerator is a nonlinear, fast-acting, multivariable system, and is usually connected through a transmission system to the rest of the power system. Turbogenerators operate over a wide range of varying conditions. Their dynamic characteristics vary as conditions change, but the outputs have to be co-ordinated so as to satisfy the requirements of power system operation. Conventional Automatic Voltage Regulators (AVR) and turbine governors are designed to control, in some optimal fashion, the turbogenerator around one operating point; at any other point the generator's performance is degraded [1].

Various techniques have been developed to design generic controllers for unknown turbogenerator systems [2]. Most adaptive control algorithms use linear models, with certain assumptions of types of noise and possible disturbances. Based on these models, traditional techniques of

identification, system analysis and synthesis can be applied to achieve the desired performance. However, the turbogenerator system is nonlinear, with complex dynamic and transient processes, hence it cannot be completely described by such linear models. Likewise, for the design of adaptive controllers, it has to be assumed that the number of system inputs equals the number of system outputs. Where necessary this is achieved by using a transformation to reduce the dimensions of the output space, with the drawback that this degrades the description of the system dynamics. Consequently, the issues of unmodelled dynamics and robustness arise in practical applications of these adaptive control algorithms and hence supervisory control is required.

Artificial neural networks offer an alternative for generic controllers. They are good at identifying and controlling nonlinear systems [3]. They are suitable for multi-variable applications, where they can easily identify the interactions between the inputs and outputs. It has been shown that a multilayer feedforward neural network using deviation signals as inputs can identify [4] the complex and nonlinear dynamics of a single machine infinite bus configuration with sufficient accuracy to then be used to design a generic controller which yields optimal dynamic system response irrespective of the load and system configurations. Numerous publications have reported on the design of ANN controllers for turbogenerators, and presented both simulation [5] and experimental results [6] showing that ANNs have the potential to replace traditional controllers.

This paper presents the design and implementation of a COT ANN controller on a laboratory turbogenerator system which is an extension of work presented in reference [5]. Experimental results are presented which compares the performance of the ANN system against a traditional AVR and governor system.

Laboratory Power System

The physical power system model in the laboratory as shown in figure 1 consists of a micro-alternator driven by a dc motor whose torque - speed characteristics are modified by a turbine simulator to behave like a turbine, and a single short transmission line which links the micro-alternator to an infinite bus.

The 3 kW, 220 V, three phase micro-alternator was designed to have all its per-unit parameters, except the field winding resistance, the same as those normally expected of a 30-1000 MW alternator. The micro-alternator parameters determined by the IEEE standards are given in Table 1 [7]. A time constant regulator is used to insert negative resistance in series with the field winding circuit, in order to reduce the actual field winding resistance to the correct per-unit value.

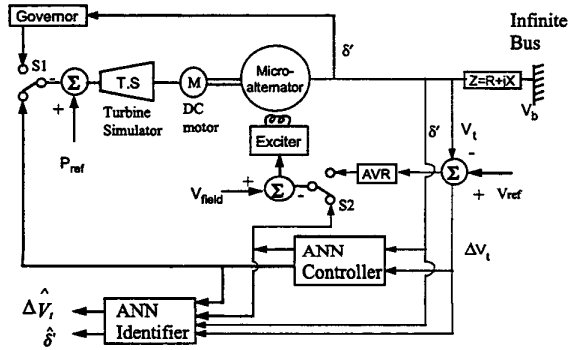


Figure 1: Physical Laboratory Model of a Power System

Table 1: Micro-Alternator Parameters

$T_{d0}' = 6.69$ s	$T_{q0}'' = 0.25$ s	$X_d' = 0.205$ pu
$T_d' = 0.66$ s	$T_q'' = 27$ ms	$X_d'' = 0.164$ pu
$T_{d0}'' = 33$ ms	$T_{kd} = 38$ ms	$X_q = 1.98$ pu
$T_d'' = 26.4$ ms	$X_d = 2.09$ pu	$X_q'' = 0.213$ pu

The traditional AVR and exciter combination transfer function block diagram is shown in figure 2 and the time constants are given in Table 2. The exciter saturation factor S_e is given by

$$S_e = 0.6093 \exp(0.2165V_{fd}) \quad (1)$$

T_{v1} , T_{v2} , T_{v3} and T_{v4} are the time constants of the PID voltage regulator compensator; T_{v5} is the input filter time constant; T_e is the exciter time constant; K_{av} is the AVR gain; V_{fdm} is the exciter ceiling; and, V_{ma} and V_{mi} are the AVR maximum and minimum ceilings.

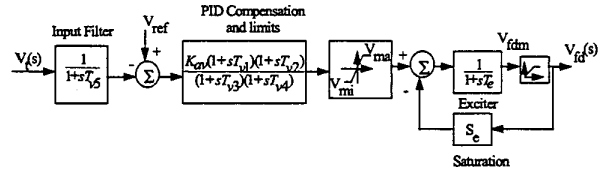


Figure 2: Block Diagram of the AVR and Exciter Combination

Table 2: AVR and Exciter Time Constants

Time Constant	Actual Value (s)
T_{v1}	0.616
T_{v2}	2.266
T_{v3}	0.189
T_{v4}	0.039
T_{v5}	0.0235
T_e	0.47

A separately excited 5.6 kW dc motor is used as a prime mover to drive the micro-alternator. The torque-speed characteristics of the dc motor is modified to follow a family of rectangular hyperbola for different positions of the steam valve. The dc motor and its associated turbine simulator circuitry represents a typical high pressure (HP) turbine cylinder. The three low pressure (LP) cylinder inertias are represented by appropriately scaled flywheels. The turbine simulator and governor combination transfer function block diagram is shown in figure 3, where, P_{ref} is the turbine input power set point value, P_m is the turbine output power, and $p\delta$ is the speed deviation. The turbine and governor time constants are given in Table 3.

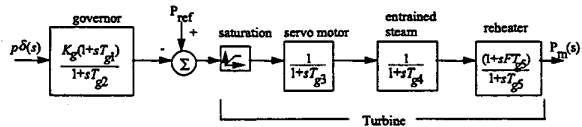


Figure 3: Block Diagram of the Turbine Simulator and Governor Combination

Table 3: Turbine and Governor Time Constants

Time Constant	Actual Value (s)
Phase advance compensation, T_{g1}	0.264
Phase advance compensation, T_{g2}	0.0264
Servo time constant, T_{g3}	0.15
Entrained steam delay, T_{g4}	0.594
Steam reheat time constant, T_{g5}	2.662
pu shaft output ahead of reheater, F	0.322

Transmission lines are modeled using the laboratory transmission line simulator, which consists of a bank of lumped inductors and capacitors.

The laboratory system was modeled in MATLAB/SIMULINK to carry out the simulation studies and details of this can be found in reference [5].

Artificial Neural Network Controller

The neural network architecture consists of two separate ANNs, namely one for the *identifier* and one for the *controller*. The identifier is used for the dynamic modelling, and the controller is used to replace the automatic voltage regulator and the governor used in conventional controllers.

Figure 4 shows a schematic diagram of the ANN two stage architecture used to implement the turbogenerator controller. This network architecture overcomes the difficulty of backpropagating errors at the turbogenerator output, across the turbogenerator to the ANN controller, during the training phase.

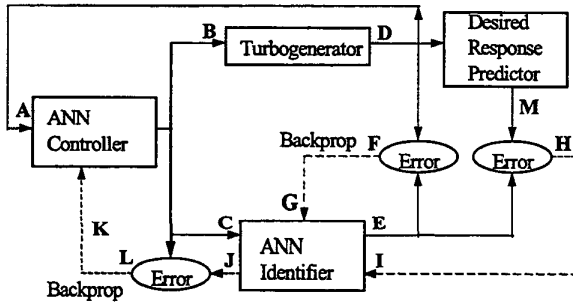


Figure 4 Neural Network Identifier and Controller Architecture

The operation of the architecture shown in figure 4 is summarised below:

- (a) The terminal voltage and speed deviations from their set points for the turbogenerator are sampled at D and time delayed.
- (b) The sampled signals from (a) are input at A to the controller ANN and the controller calculates the damping signals for the turbogenerator.
- (c) The damping signals from (b) are input at B to the turbogenerator and the same damping signals plus the signals from (a) are input to the ANN identifier at C.
- (d) The output of the turbogenerator D and ANN identifier E are subtracted to produce a first error signal F which, via backpropagation at G, is used to update the weights in the ANN identifier.

- (e) Steps (b) and (c) are now repeated using the same signal values obtained in step (a), and the output of the ANN identifier at E and the desired output at M are subtracted to produce a second error signal at H.
- (f) The error signal from (e) is backpropagated at I through the ANN identifier and obtained at J without changing the weights in the ANN identifier.
- (g) The backpropagated signals J from (f) are subtracted from the output signals of the ANN controller to produce error signals K.
- (h) The error signals at L from step (g) are used to update the weights in the ANN controller, using the backpropagation algorithm.
- (i) New control signals are calculated using the updated weights in step (h) and are applied to the turbogenerator at B again, to provide the required damping.
- (j) Steps (a) to (i) are repeated for all subsequent time periods.

The ANN identifier in figure 4 is required to produce the error signals K, which are used to update the weights in the ANN controller. With the use of this ANN identifier the need to know the turbogenerator Jacobian is avoided. Also, with the use of the ANN identifier, the ANN controller becomes adaptive and thus accurately controls the turbogenerator under all operating conditions.

A. ANN Identifier Architecture

The ANN identifier structure is fixed as a three layer feedforward neural network with twelve inputs, a single hidden layer with fourteen neurons and two outputs. The inputs are the *actual* deviation in the input to the exciter, the *actual* deviation in the input to the turbine, the *actual* terminal voltage deviation and the *actual* speed deviation of the generator. These four inputs are time delayed by a sample period of 20 ms and together with the eight previously delayed values form the twelve inputs for the model. The ANN model outputs are the *estimated* terminal voltage deviation and *estimated* speed deviation of the turbogenerator.

B. ANN Controller Architecture

The second ANN forms the controller and is a three layer feedforward neural network with six inputs, a single hidden layer with ten neurons and two outputs. The inputs are the turbogenerator's *actual* speed and *actual* terminal voltage deviations. Each of these inputs is time delayed by 20 ms and, together with four previously delayed values, form the six inputs. The two outputs of the ANN controller, the *deviation* in the field voltage and the *deviation* in the power signal, augments the inputs to the turbogenerator's exciter and turbine simulator respectively.

Implementation of the ANN Controller

The practical implementation is carried out in three stages on an IBM compatible PC with an Intel 486 based microprocessor using the standard 16-bit C language. The first stage involves the training of the ANN identifier and to verify if the ANN identifier can track the micro-alternator dynamics accurately [4]. The second stage involves the training of the ANN identifier and controller in cascade and to verify if the controller is able to predict the correct control signals. The third stage involves training and testing the ANN identifier and controller together online. In this paper results for the second and third stages are presented.

The inputs to the exciter and turbine simulator, and the outputs of the micro-alternator are all sampled at 50 Hz using four A/D channels of a PC-30 data acquisition card. The outputs of the A/D channels form the inputs to the ANN identifier and controller. The outputs of the ANN controller are passed through two D/A channels on the PC-30 card and added to the exciter and the turbine simulator reference signals.

The practical training signals for the ANN identifier and controller is similar to those used in the simulation studies [5]. A training signal with magnitudes of $\pm 15\%$ of the reference field voltage is applied to the exciter, and a training signal with magnitudes of $\pm 10\%$ of the reference power shown in figure 5 is applied to the turbine simulator.

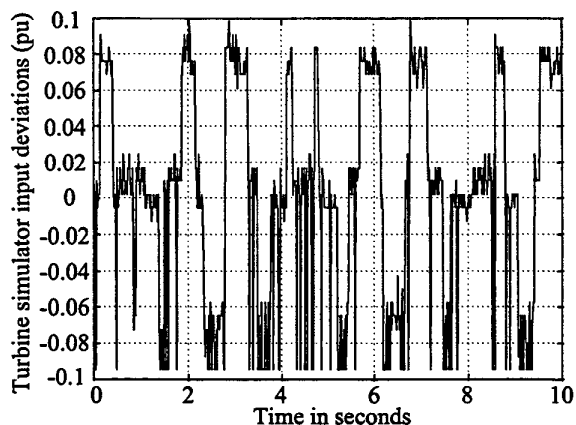


Figure 5: Practical Training Signal Applied to the Turbine

Experimental Results

The ANN controller learning curves during the training stage of the controller are shown in figures 6 and 7. After 15 s of training the controller has learned the desired control signals to damp the micro-alternator.

The dynamic and transient operation of the ANN controller is compared with the operation of the conventional controller (AVR and turbine governor) under different operating conditions such as step changes in the terminal voltage setpoint with lagging and leading power factors.

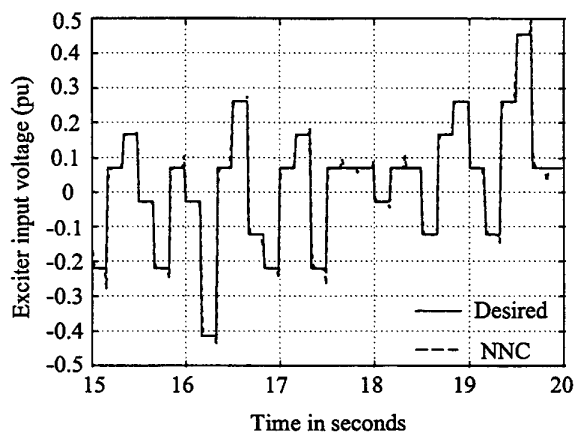


Figure 6: ANN Controller Learning the Exciter Input Signal

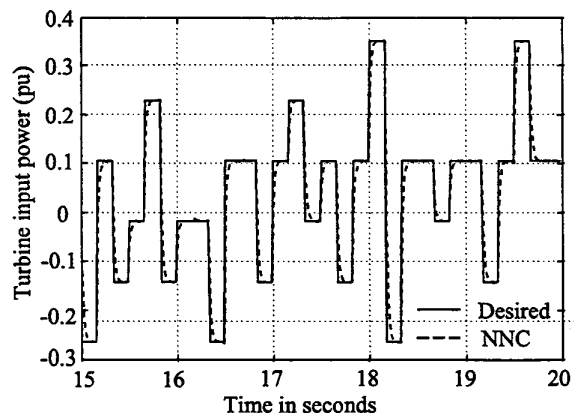


Figure 7: ANN Controller Learning the Turbine Simulator Input Signal

Figure 8 compares the load angle of the micro-alternator controlled with the conventional controller (CONV) against the result of the ANN controller (NNC) under steady state operating conditions (real power, $P = 0.4$ pu and reactive power, $Q = 0.1$ pu with a lagging power factor). The conventional controller is designed to control the turbogenerator in an optimal fashion around the operating point $P = 0.4$ pu and $Q = 0.1$ pu using the procedures similar to that in reference [8].

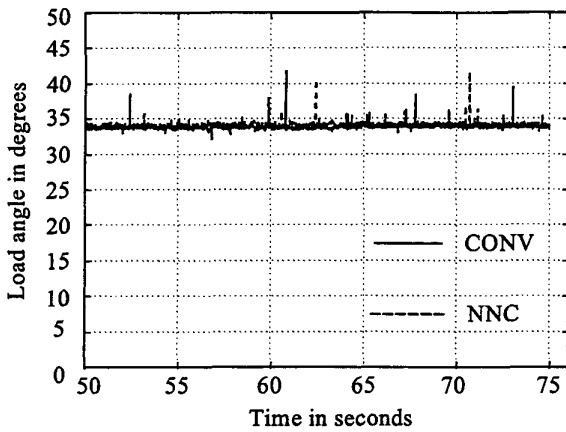


Figure 8: Load Angle of the Micro-Alternator ($P = 0.1$ pu & $Q = 0.1$ pu)

Figures 9 and 10 contain the terminal voltage of the micro-alternator with the conventional and the ANN controller respectively for a $\pm 5\%$ step change in the desired terminal voltage V_{ref} at $P = 0.4$ pu and $Q = 0.1$ pu. Figures 11 and 12 show the load angle corresponding to figures 9 and 10 respectively.

The results of figures 9 and 10 show that the terminal voltage response of the ANN controller is similar to that of the conventional controller. In the case of the load angle, figures 11 and 12 show that the conventional controller has a better response than the ANN controller during the first step change. However, the ANN controller improves its performance on the second step change as a result of *continual online training*.

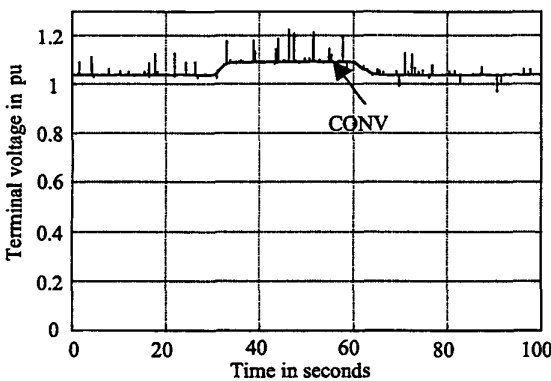


Figure 9: $\pm 5\%$ Step Changes in Desired Terminal Voltage at $P = 0.4$ pu and $Q = 0.1$ pu with the Conventional Controller

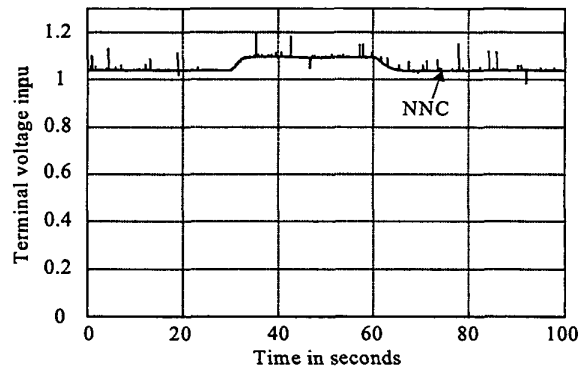


Figure 10: $\pm 5\%$ Step Changes in Desired Terminal Voltage at $P = 0.4$ pu and $Q = 0.1$ pu with the ANN Controller

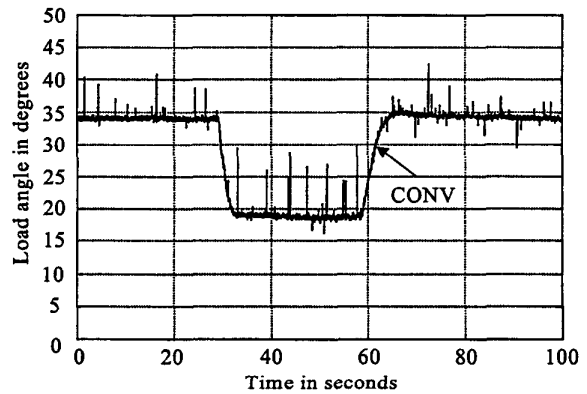


Figure 11: Load Angle for $\pm 5\%$ Step Changes in Desired Terminal Voltage at $P = 0.4$ pu and $Q = 0.1$ pu with the Conventional Controller

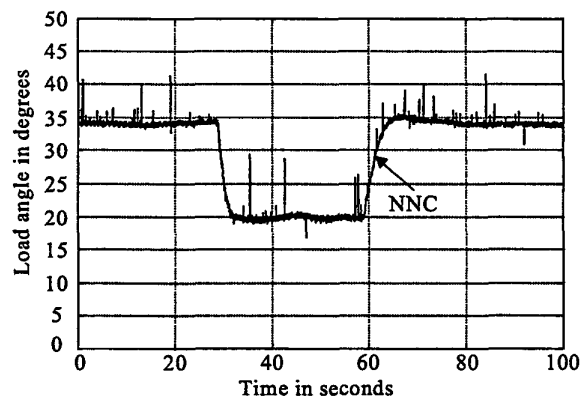


Figure 12: Load Angle for $\pm 5\%$ Step Changes in Desired Terminal Voltage at $P = 0.4$ pu and $Q = 0.1$ pu with the ANN Controller

The operating point of the micro-alternator is now changed from $P = 0.4$ pu and $Q = 0.1$ pu with a lagging power factor, to $P = 0.4$ pu and $Q = -0.4$ pu with a leading power factor. Figures 13 and 14 show the load angle of the micro-alternator for $\pm 5\%$ step changes in the desired terminal voltage V_{ref} .

The terminal voltage responses at this operating point are similar for both the conventional and ANN controller although not shown. However, figures 13 and 14 (load angles) show that the ANN controller has a smaller overshoot on the second step than with the conventional controller.

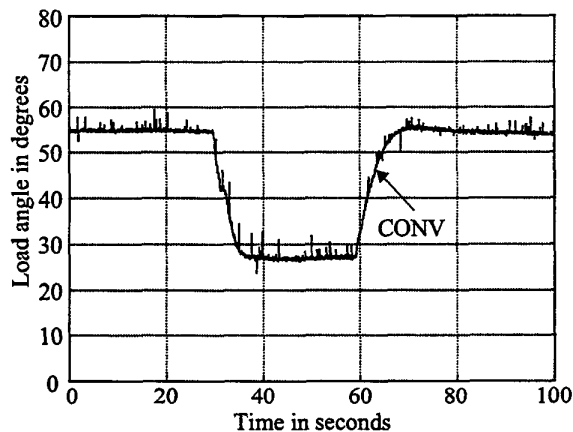


Figure 13: Load Angle for $\pm 5\%$ Step Changes in Desired Terminal Voltage at $P = 0.4$ pu and $Q = -0.4$ pu with the Conventional Controller

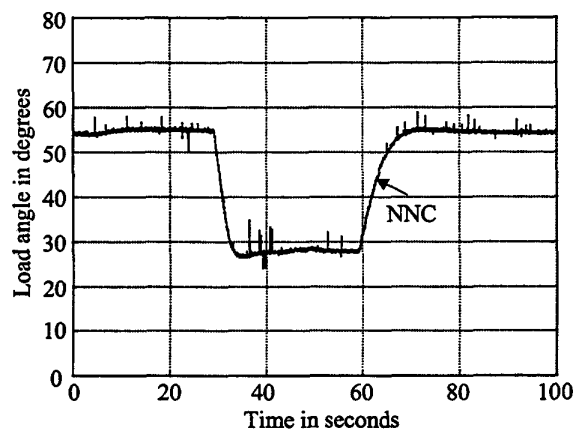


Figure 14: Load Angle for $\pm 5\%$ Step Changes in Desired Terminal Voltage at $P = 0.4$ pu and $Q = -0.4$ pu with the ANN Controller

The ANN controller is also tested at different operating points with up to $\pm 9\%$ step changes in the desired terminal voltage V_{ref} . The performance is comparable to the conventional controller, but with smaller overshoots.

Conclusions

These experimental studies on the practical implementation of a COT ANN controller show that two COT ANNs can identify and control a laboratory turbogenerator system as well as a conventional automatic voltage regulator and governor combination, when the network configuration and system operating point conforms to that for which the conventional automatic voltage regulator and governor were tuned. However, when the system conditions change, such as different power levels, the ANN identifier and controller track these changes and do not give a degraded performance as the conventional automatic voltage regulator and governor do. This superior performance of the COT ANNs occurs because the *online training never stops*. Another important consideration is that the ANNs have no prior information of the turbogenerator, need no tuning on site during commissioning, and are therefore self-commissioning.

References

- [1] Adkins B, Harley RG, "The general theory of alternating current machines", *Chapman and Hall*, London, 1975, ISBN 0-412-15560-5.
- [2] Wu QH, Hogg BW, "Adaptive controller for a turbogenerator system", *IEE Proceedings*, Vol 135, Pt D, No 1, 1988, pp 35 - 42.
- [3] Hunt KJ, Sbarbaro D, Zbikowski R, Gawthrop PJ, "Neural networks for control systems - a survey", *Automatica*, Vol 28, No 6, 1992, pp 1083 - 1112.
- [4] Venayagamoorthy GK, Harley RG, "A continually online trained artificial neural network identifier for a turbogenerator", accepted for publication in the *Proceedings of IEEE International Electric Machines and Drives Conference IEMDC'99*, Seattle, USA, 9 - 12 May, 1999.
- [5] Venayagamoorthy GK, Harley RG, "Simulation studies with a continuously online trained artificial neural network controller for a micro-turbogenerator", *Proceedings of IEE International Conference on Simulation*, University of York, UK, 30 September - 2 October 1998, pp 405 - 412.
- [6] Flynn D, McLoone S, Irwin GW, Brown MD, Swidenbank E, Hogg BW, "Neural control of turbogenerator systems", *Automatica*, Vol 33, No 11, 1997, pp 1961 - 1973.
- [7] Limebeer DJN, Harley RG, Lahoud MA, "A laboratory system for investigating subsynchronous", paper A80-0190-0, *IEEE PES Winter Power Meeting*, New York, Feb 4-8, 1980.
- [8] Ho WK, Hang CC, Cao LS, "Tuning of PID controllers based on gain and phase margin specifications", *Proceedings of the 12th Triennial World Congress on Automatic Control*, Sydney, Australia, July 1993, pp 199-202.